Adsorbing Materials for Fluoride Removal

Subjects: Materials Science, Composites

Contributor: Natalia Manousi , Ioannis Katsoyiannis , Athanasia K. Tolkou

In recent years, there has been an increase in public perception of the detrimental side-effects of fluoride to human health due to its effects on teeth and bones. Today, there is a plethora of techniques available for the removal of fluoride from drinking water. Among them, adsorption is a very prospective method because of its handy operation, cost efficiency, and high selectivity.

activated carbon adsorbents fluoride graphene oxide colorimetric sensors fluorescence sensors

1. Introduction

Fluoride ions are the negatively charged species of fluorine that occur in a plethora of minerals which can be present both in water and soil. Although there have been some reports of the possible beneficial effects of low concentrations of fluoride on dental health, especially when considered as an effective means of preventing dental caries [1], the exposure to excessive fluoride concentrations can cause severe damages to human health [1]. The negative effects of extensive fluoride exposure include dental and skeletal fluorosis, endocrine effects, attention deficit hyperactivity disorder, and neurotoxicity [2]. The margin between the desired and the undesired fluoride dose is narrow and there is therefore a great need to supervise and evaluate the quality of drinking water and, when necessary, to remove the excess of fluoride from water in order to protect human health [1][3]. **Table 1** summarizes the acceptable concentration values of fluoride in drinking water and the health effects associated with those concentration levels.

Table 1. Fluoride health effect associated with concentration levels and permissible limits of fluoride in drinking water according to the International Standards organization [4][5].

Fluoride Concentration (mg L^{-1})	Effects	International Standards Organization	Permissible Limit (mg L^{-1})
<0.5	Prevention of teeth cavities	World Health Organization (WHO)	0.6–1.5
0.5–1.5	Helps in bones and teeth development	Bureau of Indian Standards (BIS)	0.6–1.5
1.5–4	Dental problems in children	US Public Health Standards	0.8

Fluoride Concentration (mg L^{-1})	Effects	International Standards Organization	Permissible Limit (mg L^{-1})
>4	Dental and skeleton fluorosis	Indian Council of Medical Research (ICMR)	1.0
>10	Crippling skeletal fluorosis, possibly cancer	Directive 98/83/EC [6]	1.5

ses where groundwater presents unacceptable contamination levels and cannot be used without treatment for potable purposes. The fluoride contamination of drinking water is an environmental issue concerning a big part of the global population. In particular, in countries such as India, Bangladesh, China, Pakistan, Ghana, and Tanzania [7][8], the concentrations of fluoride in the waters are so high that several thousands of people suffer from fluoride associated illnesses. Effective fluoride removal in these regions is thought to be a difficult and stimulating matter, mainly due to the difficulties arising from fluoride chemistry which prevent fluoride from being efficiently sorbed by most conventional adsorbents used in the drinking water industry. A lack of essential infrastructure and technological know-how also play a significant part. [7][9]. However, China [10] and India [11] are making efforts to defeat this problem and the situation is constantly improving.

Consequently, fluoride removal from drinking water has received great attention in the last years and several technologies have been tested in laboratories or applied in the field [12][13][14][15]. Ion exchange, chemical precipitation, membrane processes, coagulation, adsorption and both phyto and bio-remediation are the main technologies which have already applied for the removal of fluoride in potable water treatment. **Figure 1** summarizes the commonly applied techniques and their main advantages and disadvantages.

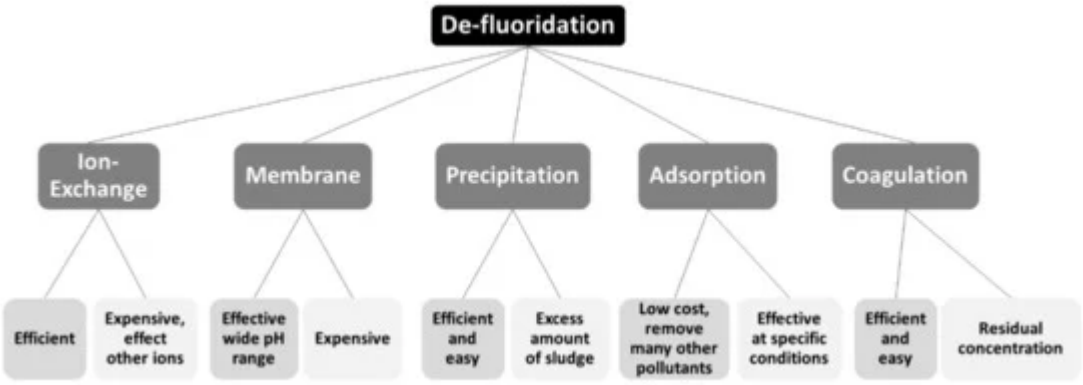

Figure 1. Commonly applied techniques for fluoride removal from drinking water [16][17][18][19].

Nevertheless, most of the aforementioned methods display particular disadvantages. In the case of ion-exchange, the price of resin, its regeneration and resultant waste disposal requirements, and the fact that it is not selective enough preclude this method from being efficient and cost-effective [18]. The use of membranes belongs to the same category of disadvantages, as the elevated cost of membrane acquisition and operation and the disposal of concentrates, which necessitates posttreatment of water, makes the process rather uneconomical [20]. Coagulation, on the other hand, is an economical technology for defluoridation but requires high doses, leading in high residual concentrations, (e.g., of harmful aluminum) and hence produces significant amounts of sludge [17]. Precipitation

methods relying on the use of calcium, aluminum, and iron salts have been widely published in the literature as well. Nevertheless, the problems related to lime-based processes include the low solubility of the resulting calciumhydroxide, which hinders adequate removal of fluoride from the waters [17][18]. Among these processes, adsorption is a very promising technique due to its handy operation, low-cost operation, increased selectivity, and the readiness of adsorbents. Materials such as alumina [16], activated carbon [21], ion exchange resins [22], silica gel [23], natural materials such as clay [24] and mud [25][26], and low-cost alternative adsorbents such as fly ash [27][28], bone charcoal [29], metallic iron [30], nanomaterials [31][32], etc., have been employed [12][13][14].

In parallel, due to its profound effect on human teeth and bones, there is a demand for the development of precise and sensitive analytical methods for the measurement of fluoride in aquatic solutions. Until recently, several methods have been developed to determine fluoride in drinking water. These methods were classified into six main categories [33], namely chromatographic, electrochemical and spectroscopic methods, microfluidic analysis, titration, and sensors. Among the chromatographic methods, high-performance liquid chromatography (HPLC), ion chromatography (IC), and gas chromatography (GC) are the most widely used techniques for fluoride determination. Electrochemical methods include potentiometry, ion selective potentiometry, polarography, and voltammetry. Spectroscopic methods include atomic and molecular spectroscopy, while microfluidic analysis includes flow injection analysis (FIA) and sequential injection analysis (SIA) [33][34]. Up to date, the development of novel cost-efficient fluoride monitoring systems for the assessment of drinking water quality has been undoubtedly at the forefront of research [33][35].

There is a number of review articles in the literature regarding the removal [3][36][37] and the analytical determination [33][36] of fluoride from various matrices. Herein, the methodology that we followed to prepare this review study was based on the presentation and the discussion of recently developed materials (mainly adsorptive materials) in order to highlight the specific properties which enhance fluoride removal. Novel adsorbents have been classified in the following categories: carbon-based materials (i.e., activated carbon (AC), graphene oxide (GO) and carbon nanotubes (CNTs)); nanostructured materials combining metals and their oxides or hydroxides; and natural materials. These adsorbents have been reviewed and critically assessed. Regarding analytical techniques, the most common techniques for fluoride determination are presented, and an emphasis has been given to methodologies developed between 2015 and 2021. The novelty of this review is based on the fact that the most recent reviews for fluoride removal have only reported, in general, on the technologies used for removal and have not focused on newly produced adsorbing materials. To the best of our knowledge, this is the first review which also combines the relevant analytical techniques required for fast and accurate fluoride determination. The further objective of the present study is to compare and identify possible new materials with high advantages for fluoride removal with the aim of producing an adsorbent with high efficiency for fluoride removal which will also be able to be placed in the market.

2. Fluoride Removal from Drinking Water by Adsorption

In this section, the recently developed adsorbing materials for fluoride removal from water are categorized as follows: carbon-based materials (i.e., AC, GO and CNTs) and other nanostructured materials. The following is a

description of the basic characteristics of several recently developed materials. In **Table 2**, these are summarized and their characteristics are compared.

2.1. Carbon-Based Adsorbents

Carbon-based materials have been proved to be very beneficial in the potabilization of water since they demonstrate outstanding adsorption characteristics. Research findings have shown that activated carbon, graphene oxide, and carbon nanotube have plentiful surface functional groups and substantial specific surface areas [37]. The aim of this section is to summarize and assess carbon-based materials for de-fluoridation of water on the basis of their effectiveness, cost-effectiveness, and readiness for application [5].

Currently, one of the most widely applied carbon-based materials for fluoride removal is bone char (BC), which is considered as a conventional treatment [38] with very good reported removal efficiencies [39] and, in some cases, is considered as a green sorbent [40]. Bone char is a material comprised of carbonated and inorganic materials (70–76% of hydroxyapatite (HAP,$Ca_{10}(PO_4)_6(OH)_2$)) that has been successfully utilized to decrease the content of fluoride in water [41][42]. Several recent studies [29][43][44][45][46], have reported very high adsorption capacities (i.e., 11.2 mg F^- g^{-1} for Chicken Bone Char (CBC)) [45]. However, the use of bone char and its application for de-fluoridation can be hindered by the traditions and religious attitudes of people (i.e., char derived from cow bones is not tolerable by Hindus and, likewise, pig's bone char is not acceptable by Muslims) [40]. In addition, the use of low-grade bone char adds bad taste and odor to the treated water. Moreover, owing to the numerous reviews that already exist specifically for bone char application for the de-fluoridation of waters, bone char is not further examined in detail in this review.

2.1.1. Activated Carbon

AC is a common adsorptive material, used for removing pollutants from water sources due to its enhanced porosity, significant surface area, and also its adaptable surface chemistry [47]. Modified activated carbon materials with the oxides and hydroxides of metals have been used to expand its available surface area [48] and to strengthen its interactions with fluoride [49].

Activated Carbon Fibers Modified with Zirconium (Zr-ACF)

In the study conducted by Pang et al. [50], a new drop-coating method was created to prepare Zr-ACF adsorbents for fluoride removal. Adsorption trials at pH values between 3 and 11 showed that ion exchange and electrostatic attraction were the main mechanisms of fluoride retention. The pseudo-second-order model (PSO) describes properly the kinetics of fluoride adsorption, and the Langmuir model f fitted well to the isotherms data. The highest adsorption capability was 28.50 mg L^{-1}.The thermodynamic study indicated that the adsorption process of fluoride onto Zr-ACF is endothermic and spontaneous, as indicated by the negative value of Gibbs energy (ΔG°) [51][52] and the positive value of enthalpy (ΔH°) [53], respectively. The results indicated that Zr-ACF made by drop-coating is a cost-effective and high-capacity adsorbent for fluoride removal due to its simplicity of synthesis and enhanced adsorption capacity.

Activated Carbon of Avocado Seeds (ACAS)

The study conducted by Tefera et al. [54] investigated the performance of ACAS for fluoride removal from aqueous solutions and groundwaters. Adsorption of fluoride onto ACAS reached its equilibrium condition at the contact time of 60 min at pH 6 and an ACAS dose of 19 g L^{-1} with a fluoride starting concentration of 5.2 mg L^{-1}. The experimental data were well fitted to the Langmuir isotherm model with a highest adsorption capability of 1.2 mg g^{-1}.

Activated Carbon Derived from $CaCl_2$-Modified Crocus Sativus Leaves (AC-CMCSL)

Fluoride adsorption by AC-CMCSL [55], at its best conditions (i.e., an influent fluoride concentration of 6.5 mg L^{-1}, pH value of 4.5, adsorbent dose of 15 g L^{-1}, and reaction time of 70 min) showed a maximum adsorption capacity of 2.01 mg g^{-1}. The results fit well with the Langmuir model. In addition, the impact of the co-occurring anions on fluoride sorption was examined, and their effect is reflected in the following order: PO_4^{3-} > SO_4^{2-} > Cl^- > NO_3^-. The findings of the presented study showed that AC-CMCSL has a moderate ability for fluoride removal from waters. The thermodynamic parameters calculated in this study confirmed the endothermic nature of the adsorption on AC-CMCS, indicated by a positive value of ΔH° (+22.6 kJ mol^{-1}) and the fact that the adsorption of fluoride on AC-CMCSL was spontaneous, as all ΔG° values were negative for all the studied temperatures (i.e., −0.20576 kJ mol^{-1} at 303 K).

La/Mg/Si-Activated Carbon

La/Mg/Si-AC, originating from palm shells, was recently studied and was found to be an appropriate material for eliminating fluoride from natural waters [56]. It is worth noting that La/Mg/Si-AC has a rough and porous structure, homogeneously modified by impregnation with La, Mg, and Si. This material was found to be applied to the concurrent removal of aluminum and fluoride from solutions. The adsorption process of fluoride is driven by an endothermic (ΔH° = +7.5 × 10^3 kJ mol^{-1}) and spontaneous (ΔG° = −1.41 × 10^4 kJ mol^{-1} at 308 K) reaction and was more favored at acidic pH values than the point of zero charge of La/Mg/Si-AC (pH_{pzc} 9.6) with a high temperature.

A schematic presentation of the relative presented activated carbon materials used for fluoride removal is illustrated in **Figure 2** showing the modification type, the optimum pH value for adsorption, the maximum adsorption capacity, and the contact time of adsorption.

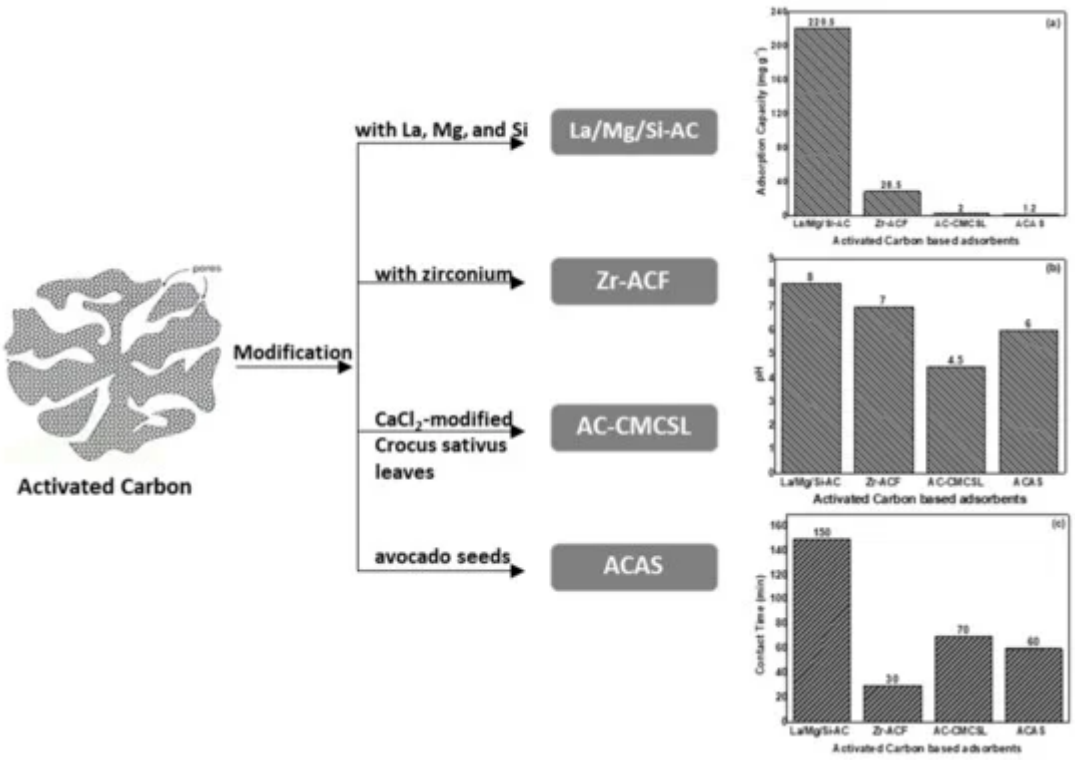

Figure 2. Schematic presentation of modified activated carbon-based materials used for fluoride removal, showing (**a**) the pH optimum activity, (**b**) the maximum adsorption capacity, and (**c**) the contact time of adsorption.

In more detail, **Figure 3** shows, in descending order, the maximum adsorption capacity (mg g^{-1}) of the modified activated carbon materials presented in this study. As depicted, La/Mg/Si-AC exhibited the highest capacity (220.5 mg g^{-1}) among them.

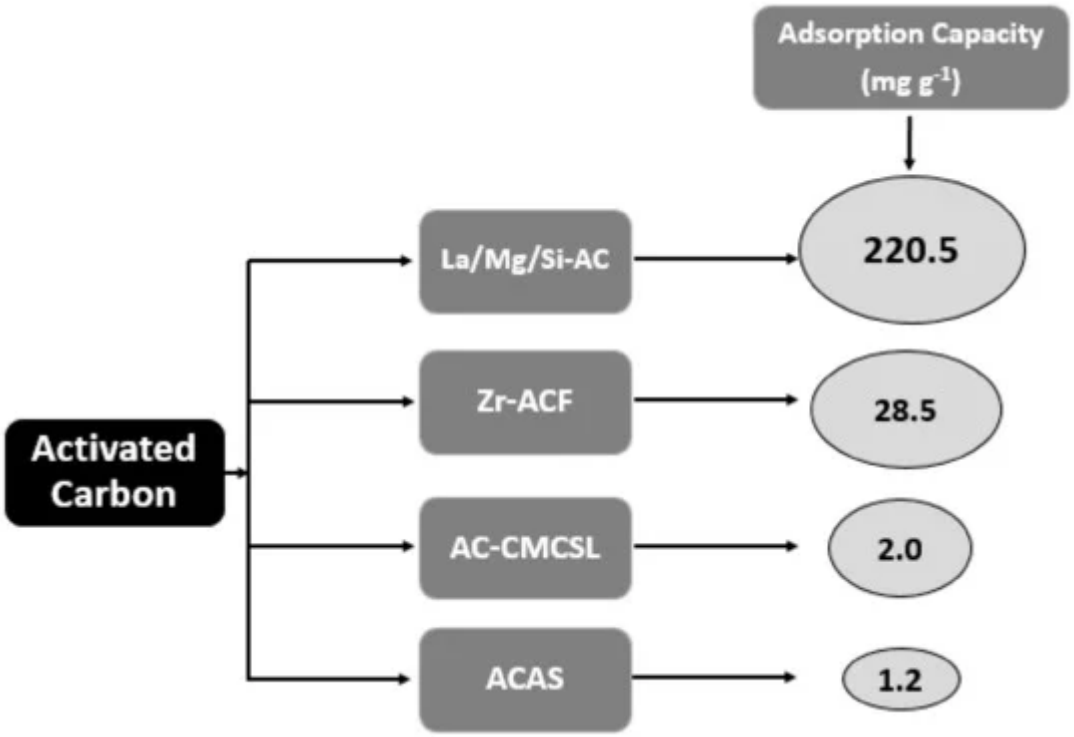

Figure 3. Schematic graph of depicting maximum adsorption capacities (mg g^{-1}) of presented activated carbon-based materials.

2.1.2. Graphene Oxide

Recently, GO has been widely effectively applied in water treatment [57][58]. However, pure GO materials show inadequate adsorption ability. Besides, they are very slight and stable in water, making them very challenging to recover after adsorption. One efficient way to overcome this challenge is to amend its surface [59]. Considerable research studies in this direction have been dedicated to changing the local reactivity via doping or grafting elements such as Al, Mn, Fe, Mg, Au, Ti, B, and Si [60][61] among others.

Graphene Oxide/Alumina Nano-Composite

GO/Al_2O_3 was produced with GO and γ-Al_2O_3 by using a hydrothermal reaction. This arrangement was accomplished by creating hydrogen bonds between hydroxyl and carboxyl functional groups on the surface of γ-Al_2O_3 and GO nanosheets [62]. The presence of GO enlarged the specific surface area of the newly created material. As a result, the fluoride adsorption rate was fast during the first 60 min, and the adsorption equilibrium state was achieved at about 90 min of reaction. The findings demonstrated that the sorption capacity (4.68 mg g^{-1}) of GO/Al_2O_3 is greater than that of γ-Al_2O_3 (3.04 mg g^{-1}). Adsorption kinetics was found to follow the pseudo-second-order model, which suggests fluoride removal via chemisorption mechanism and thermodynamics showed that the fluoride adsorption behavior by GO/Al_2O_3 is spontaneous with a negative ΔG° value (−2.32 kJ mol^{-1} at 303 K). Additionally, the positive value of ΔH° (+24.6 kJ mol^{-1}) exhibited that fluoride adsorption by GO/Al_2O_3 is endothermic in nature. Furthermore, PO_4^{3-} and HCO_{3-} had a great influence on fluoride removal in an aqueous solution. The impact of the pH value on fluoride removal was relatively minor, which indicated that GO/Al_2O_3 is effective within a broad range of pH values.

Graphene Oxide–Aluminum Oxyhydroxide Interaction (GO–Al–O(OH))

The present material refers to modification of aluminum oxyhydroxide [Al–O(OH)] by graphene oxide. It was produced by a chemical precipitation wherein Al^{3+} ions interact with various functional groups of GO [63]. The maximum adsorption capacity of GO–Al–O(OH) adsorbent was 51.42 mg g^{-1} with only 2.0 g of the adsorbent placed in a laboratory scale column. Experiments were accomplished at pH 7.0, and the adsorption could be satisfactorily described by the Langmuir and Dubinin–Radushkevich isotherm models. The adsorptive rate of fluoride increased with time, providing substantial removal efficiency after 60 min. Under these conditions, fluoride residual concentration was below the legislative limit. The negative values of ΔG° (−5.84 kJ mol^{-1}, at 303 K), correspond to a spontaneous process of F ion adsorption onto the GO–Al–O(OH), while the positive value of ΔH° (+21.4 kJ mol^{-1}) indicated that the adsorption phenomenon is endothermic.

Graphene Oxide/Eggshell (GO/ES) Adsorbent

The GO/ES adsorbent has been studied for fluoride removal [64]. Eggshells are calcium-containing materials that have been used by researchers as adsorbents for F^- removal due to their solid affinity towards the pollutants of

interest. GO/ES is a material that benefits from the properties of each component for better efficiency. The maximum adsorption capacity of F^- (56 mg g^{-1}) was obtained with 25 mg L^{-1} of F^- initial concentration after 120 min of contact time with an adsorbent dosage of 0.05 g of GO/ES. Adsorption isotherms showed that the experimental data were best fitted by the Langmuir model, indicating that F^- adsorption is characterized by monolayer adsorption on a homogenous surface of GO/ES. The conducted thermodynamic study showed that, as the temperature increases, an increment in ΔG° values was recorded (from 0.1865 kJ mol^{-1} at 298 K to 2.4085 kJ mol^{-1} at 348 K), suggesting that higher temperatures render the adsorption of F^- by using GO/ES unfavorable, while the negative value of ΔH° (−12.7 kJ mol^{-1}) indicates that the adsorption process is exothermic. The disadvantage of this research is that it does not refer to the effect of pH and the presence of other ions that may affected the results.

Graphene Oxide Anchored Sand (ZIGCS) Functionalized by Zr(IV)

GO was manufactured from low-cost materials, sugar, and river sand, which were impregnated with zironium (Zr) (ZIGCS) and used for the de-fluoridation of water [65]. Unmodified GO cannot be considered as an efficient adsorbent due to the considerable aggregation of graphene oxide nano-sheets in water, which causes a significant loss of its high adsorption potential. This aggregation was effortlessly conquered via covering of sand particles by coating, which provided a cheap context for graphene oxide preparation. The reaction of F^- on ZIGCS depended on its pH values, with maximum adsorption to take place at pH 4 close to its ZPC of 4.5. However, the material was efficient enough in the whole pH range between 2 and 9. The reported Langmuir maximum adsorption capacity of 175 mg g^{-1} is an above average value, compared to the other carbon-based adsorbents studied for de-fluoridation. In this study, the increase in negative ΔG° values with a rise in temperature demonstrated that the F^- adsorption by ZIGCS is thermodynamically possible and spontaneous, suggesting a favorable adsorption at high temperatures. Moreover, a positive ΔH° value indicates that the adsorption process was endothermic.

In addition, **Figure 4** illustrates a schematic presentation of the presented modified graphene oxide-based materials, their optimum pH values, their relative adsorption capacities, and the contact time for optimized adsorption.

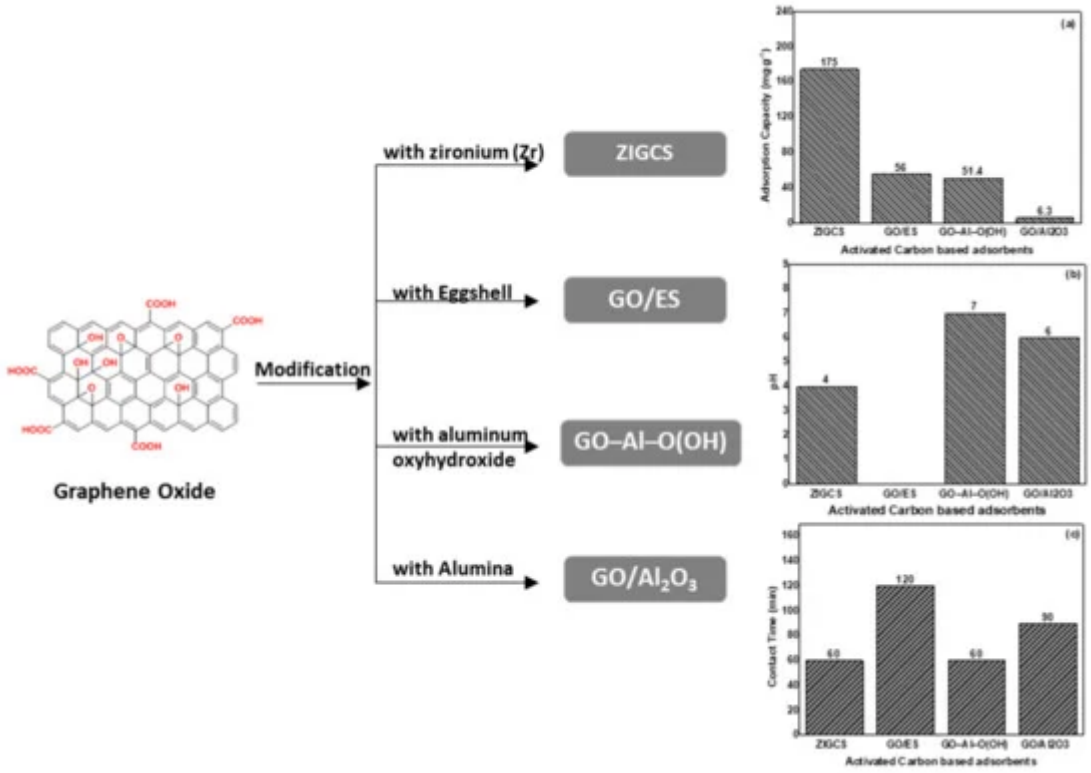

Figure 4. Schematic presentation of modified graphene oxide-based materials used for fluoride removal showing (**a**) the optimu pH optimum, (**b**) the maximum adsorption capacities, and (**c**) the contact time of adsorption.

In more detail, **Figure 5** presents the maximum adsorption capacities (mg g^{-1}) of modified graphene oxide materials. As shown, ZIGCS is the graphene-based material that presents a maximum adsorption capacity of 175 mg g^{-1}, among the other materials reviewed in this study.

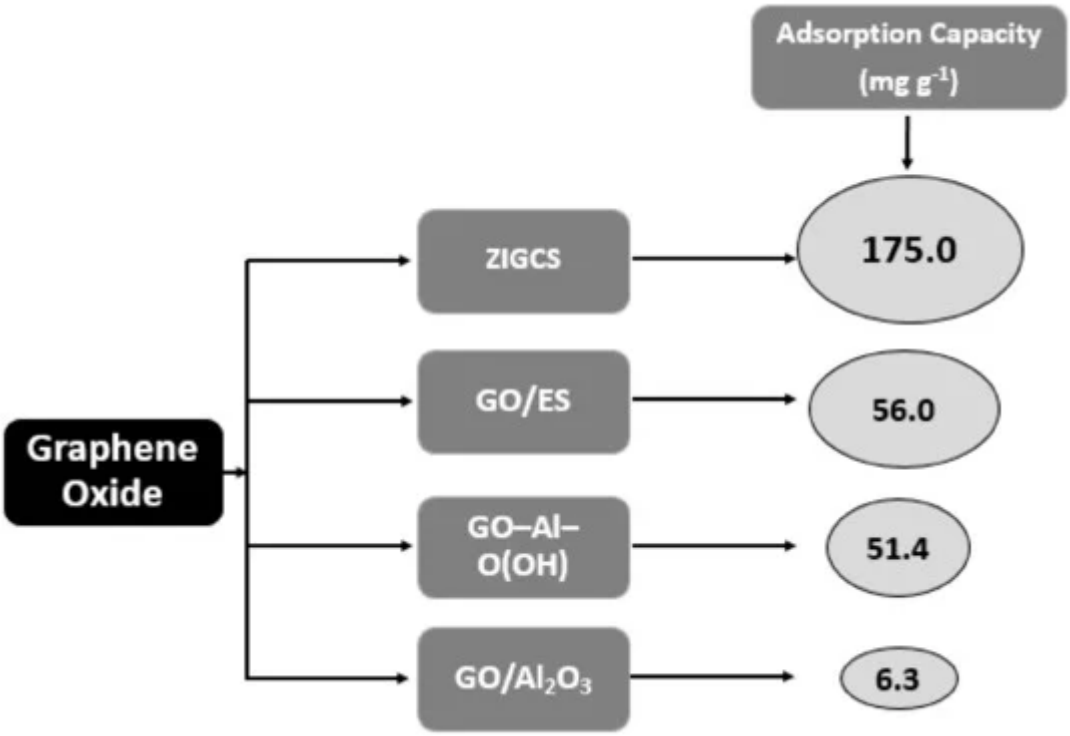

Figure 5. Schematic graph of depicting maximum adsorption capacities (mg g^{-1}) of presented graphene oxide-based materials.

2.1.3. Carbon Nanotubes (CNTs)

Carbon nanotubes, an allotrope of carbon, have uncommon features which are important in nano-technology. Furthermore, due to their potential for being functionalized by appropriate reactive groups and their one dimensional structure, the characteristics of CNTs can easily be controlled and improved [66]. In the last three years, however, there has been no extensive research into their use to remove fluoride.

Hydroxyapatite/Multi-Walled Carbon Nanotubes (HA-MWCNTs)

The production of MWCNTs was made using a simple in situ sol–gel method, and was used for the removal of fluoride from water [67]. Based on the results achieved in the study of Ruan et al. [67], HA-MWCNTs exhibited a high fluoride adsorption capacity of 39.22 mg g^{-1} at 323 K and an adsorbent dose of 2.0 g L^{-1} at pH 7.0. The adsorption reaction was spontaneous ($\Delta G° = -1.964$ kJ mol^{-1} at 303 K) and endothermic ($\Delta H° = +6.4$ kJ mol^{-1}) and appeared to occur as a result of both anion exchange and electrostatic interactions. The removal of fluoride by the composite was observed to be firmly reliant on the experimental conditions, which included temperature, contact time, solution pH, and interfering of other co-occurring anions such as HCO_3^-, CO_3^{2-}, and $C_2O_4^{2-}$. These anions exhibited the following order: K_h (CO_3^{2-}) > K_h (HCO_3^-) > K_h ($C_2O_4^{2-}$). **Figure 6** presents the major characteristics of carbon nanotube-based material applied for fluoride removal and reviewed in the present study.

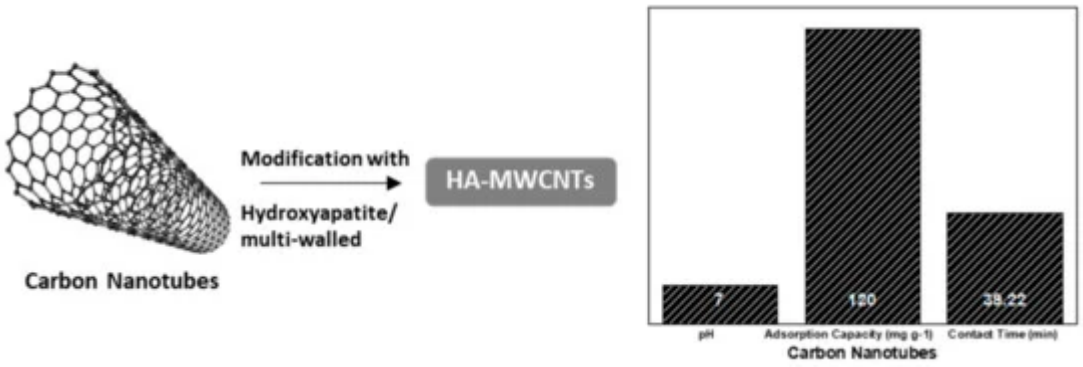

Figure 6. Schematic presentation of modified carbon nanotube-based material used for fluoride removal showing the optimum pH optimum, the maximum adsorption capacity, and the required contact time.

2.2. Other Adsorbents

Beside the use of adsorbents based on carbon, there is a broad range of new materials (mainly nanostructured) that are well applied to remove fluoride, combining metals and their oxides or hydroxides as well as natural materials.

2.2.1. SRH Adsorbent

Recently, Pillai et al. [68] synthesized a silica nano adsorbent altered by rice husk for fluoride removal, which is economic and gives a decent result with respect to fluoride removal. Various parameters affect its de-fluoridation efficiency. The results revealed a superb efficiency for fluoride removal with a reported adsorption capacity of 12 mg g^{-1}, obtained with a dose of 4 g L^{-1} corresponding to 72% fluoride removal efficiency. The result of the equilibrium data follows the Langmuir isotherm.

2.2.2. Fe@BDC and Fe@ABDC Fe-Based MOF Composites

Synthesis of Fe^{3+} fabricated BDC and ABDC provides Fe@BDC and Fe@ABDC MOF composites, which can be applied for effective de-fluoridation from aqueous solutions [69]. The improved DC of Fe@BDC and Fe@ABDC MOF composites offered an adsorption capacity of 4.90 and 4.92 mg g^{-1}, which were fitted to Langmuir isotherm model. Thermodynamic parameters exhibited that the de-fluoridation process onto Fe@BDC and Fe@ABDC MOF composites was spontaneous and feasible in nature because of negative values of ΔG° (−7.31 and −8.15 kJ mol^{-1} at 303 K, respectively). Additionally, the positive ΔH° values (+0.6 and +1.2 kJ mol^{-1} for Fe@BDC and Fe@ABDC MOF composites) exhibited the nature of fluoride adsorption process, which was considered to be an endothermic chemical adsorption. The recycle of the Fe@BDC and Fe@ABDC MOF composites were executed for six cycles.

2.2.3. Modified Kaolin–Bentonite Composites (KBNPs)

The incorporation of nanoparticles of iron oxides in kaolin–bentonite composite adsorbents for fluoride adsorption from drinking water was studied by Annan et al. [70]. The adsorption of F^- was noticed to be better described by the Freundlich isotherm model, and a pseudo-second-order kinetic model was fitted well to describe the kinetics of

adsorption. The results evidently show that the saturation of clays with magnetite nanoparticles has a considerable effect on F^- removal. The newly synthesized material showed a maximum percentage removal of 91% after a 120 min contact time. This study undoubtedly demonstrated that a sustainable approach for the design of filtration systems for the removal of fluoride from groundwater can be applied by using cheap components which are also locally accessible.

2.2.4. Ce\Zn Ceramic Oxides

Corresponding published results show that [71] the metal oxides of cerium (Ce) and manganese (Mn) produced by a precipitation method have exceptionally high fluoride sorption abilities. The synthesis of bimetallic oxides such as Al\Ce or Ce\Zn has exhibited an even higher effectiveness, mainly attributed to the elevated density of hydroxyl groups. Particularly, Ce\Mn ceramic oxide manufactured for 4 h showed a fluoride adsorption capacity of up to 257.8 mg g^{-1}. In comparison, this value is 1.6 times superior to the adsorption capacity of Ce\Mn synthesized for 1 h. Likewise, this material presented rapid kinetics with 68% of fluoride initial concentration to be retained by the adsorbent in the first 5 min, reaching equilibrium after 15 min.

2.2.5. Porous MgO Nanostructures

According to Borgohain et al. [72], the MgO nanostructures of diverse morphologies have been formulated by the sol–gel and hydrothermal method in an aqueous medium in the absence of additional templates. The MgO nanostructures are exceedingly crystalline and porous, having an elevated surface area within the range from 10.5 to 171.2 m^2 g^{-1}. Their morphology depends on the synthesis approach as well as the metal ion precursor. The kinetic studies indicated that adsorption is very fast and that the MgO nanostructures present high retention capability (varied from 5716 to 15,691 mg g^{-1} at 303 K) and follow the Langmuir model. The utmost Langmuir adsorption capacity of 29,131 mg g^{-1} has been achieved at 313 K, which is the best result between all adsorbents described until in this review. Negative value of Gibbs free energy ($\Delta G° = -21.1$ kJ mol^{-1} at 303 K) for this adsorbent, suggests a thermodynamically favorable interaction between fluoride and the adsorbent, while the negative value of $\Delta H°$ (−47.6 kJ mol^{-1}) indicates that the adsorption is an exothermic process.

2.2.6. Lanthanum Modified Mesoporous Alumina (La/MA)

The elimination of F^- from aqueous solutions utilizing La/M was examined by He et al. [73]. The Elovich kinetic model was proven to offer the best correlation for the adsorption. The highest monolayer adsorption capacity of F^- was about 26.45 mg g^{-1} in the Sips model (at a dosage of 2.0 g L^{-1}) and had slightly acidic conditions (pH = 6.0 ± 0.1). Negative values of $\Delta G°$ (i.e., −3.761 kJ mol^{-1} at 298 K) indicated that the adsorption process was feasible and spontaneous. The positive value of enthalpy (+3.9 kJ mol^{-1}) showed that the adsorption was endothermic. Still, the influence of co-existed anions on F^- removal was investigated, and it was indicated that the removal efficiency was vaguely affected by the presence of Cl^- and NO^{3-}, whereas SO_4^{2-} and CO_3^{2-} caused a sharp decrease in the removal efficiency. In the same study, while cerium modified mesoporous alumina (Ce/MA) was also analyzed for its efficiency, the La/MA was a better adsorbent than the employed Ce/MA.

2.2.7. Iron Oxide Nanoparticles Modified with Ionic Liquid (IL-Iron Oxide)

A new material, IL-iron oxide NPs was manufactured by the co-precipitation method using ionic liquids (IL) as a solvent and trihexyl(tetradecyl)phosphonium chloride [THTDP]Cl as a coating material [74]. The main part between IL-iron oxide and fluoride ion was an electrostatic attraction which concurrently enhanced the elimination of fluoride. An investigation of kinetics confirmed that fluoride elimination was enhanced rapidly during the starting period, and the highest fluoride retention efficiency was achieved in 30 min. The best isotherm model was the Langmuir model which revealed a sorption capability of 67.9 mg g^{-1} with ceiling fluoride removal of 96%. Thermodynamic results showed that ΔG° decreased with a rise in temperature (from −15.6 kJ mol^{-1} at 283 K to −60 kJ mol^{-1} at 303 K) with positive ΔH values (ΔH° = +6.6 kJ mol^{-1}) indicating the spontaneous and endothermic nature of the fluoride adsorption.

2.2.8. γ-Al_2O_3/γ-Fe_2O_3 Composite

A recyclable mesoporous magnetic adsorbent of γ-Al_2O_3/γ-Fe_2O_3 nanocomposite was produced by Roy [75] by a microwave irradiation method. Fluoride adsorption equilibrium was accomplished within 15 min and the maximum adsorption capacity of γ-Al_2O_3/γ-Fe_2O_3 nanocomposite was 105.04 mg g^{-1} at pH 7.0, which is better than several other reported adsorbents, by using 1.0 g L^{-1} of adsorbent dosage. Thermodynamics showed that the negative value of ΔG° (−27.326 kJ mol^{-1} at 303 K) and the positive value of ΔH° (+14.4 kJ mol^{-1}) suggest the adsorption process is favorable, spontaneous, and endothermic, accordingly. The adsorption process followed the Langmuir model. The nanocomposite has a superior affinity for fluoride ions in the presence of other interfering co-existing anions. Therefore, the conclusion of this study demonstrated the prospective ability of γ-Al_2O_3/γ-Fe_2O_3 nanocomposite to develop an efficient adsorbent for fluoride

2.2.9. Zirconium-Based Metal Organic Framework (MOF-801) Adsorbent

A MOF-801 adsorbent, applying a solvothermal method and investigating its adsorption effectiveness for removal of F- from water, was studied by Tan et al. [76]. The produced MOF-801 had a surface area of 522 m^2 g^{-1} and exhibited superb performance in the adsorption of fluoride from water, with an optimum adsorption amount for fluoride of up to 17.33 mg g^{-1} at a dosage of 1 g L^{-1}.The kinetic studies showed that the adsorption of fluoride is described by the Langmuir isotherm model and could be well fitted with pseudo-second-order model, hence presuming that fluoride adsorption on MOF-801 relies on chemisorption. The summarized findings implied that the synthesized MOF-801 has the ability to be an outstanding technology.

2.2.10. Biosynthetic Crystals by Microbially Induced Calcium Carbonate Precipitation (BC-ICP)

BC were made according to the process of Wang et al. [77] through microbially induced calcium carbonate precipitation (MICP) for fluoride removal from groundwaters. The findings revealed that the maximum fluoride adsorption capability and defluorination efficiency reached 5.10 mg g^{-1} and 98.24%, at pH 7.0 and a BC dose of 1.0 g L^{-1}, respectively. The fluoride adsorption on BC was observed to be a heterogeneous and multi-layered

adsorption process, principally dominated by chemisorption, and the Freundlich isotherm model better described the reaction. The mechanism that occurs in the adsorption and precipitation of fluoride by BC takes place simultaneously with the co-precipitation of Ca^{2+}, PO_4^{3-} and F^-. As the fluoride adsorbs onto the surface of BC, induced calcium ions (from calcium carbonate) precipitate into the CaF_2. As exhibited from the thermodynamics study, ΔG° decreased with the rise in temperature and the negative value of ΔG° (−4.60 kJ mol^{-1} at 303 K) indicate that the adsorption process was spontaneous and thermodynamically favorable in nature. ΔH° (+2.3 kJ mol^{-1}) had positive values, which suggested an endothermic adsorption process. The method is efficient for longer periods of operation and can be applied in full scale fluidized bed reactors.

2.2.11. Lanthanum Ferrite Nanoparticles ($LaFeO_3$ NPs)

Mesbah et al. [78] aimed to produce $LaFeO_3$ NPs and examine its efficiency on the elimination of fluoride from waters. The largest percentage removal of 94.75% fluoride on $LaFeO_3$ NPs was achieved under optimum conditions of pH of 5, $LaFeO_3$ NPs dosage of 0.9 g L, a temperature of 308 K, and a contact time of 60 min. The process of fluoride adsorption on $LaFeO_3$ NPs followed the Freundlich adsorption and Koble–Corrigan isotherm models. The negative ΔH° value of the sorption suggests that the process was exothermic. The increase in temperature resulted in an increase in spontaneity and feasibility, while the values of ΔG° were negative (i.e., −4.06 kJ mol^{-1} at 308 K).

A schematic presentation of the four most efficient presented materials is showed in **Figure 7**.

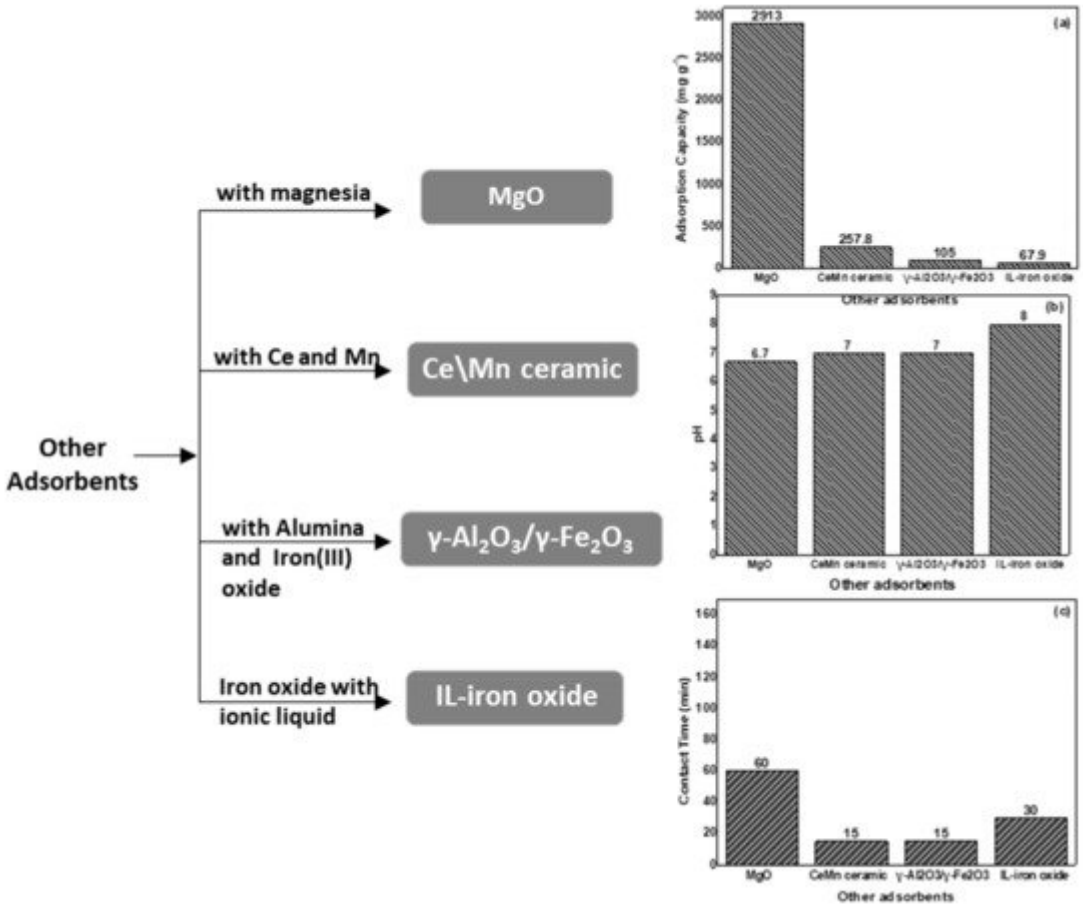

Figure 7. Schematic presentation of the four most efficient presented materials used for fluoride removal, showing the modification type, (**a**) the pH optimum activity, (**b**) the maximum adsorption capacities and the contact time (**c**) of adsorption.

In more detail, **Figure 8** shows in descending order the maximum adsorption capacities (mg g^{-1}) of the four most efficient materials. Among them, the MgO nanostructures exhibited the highest adsorption capacity (29,131 mg g^{-1}) of all of the presented materials.

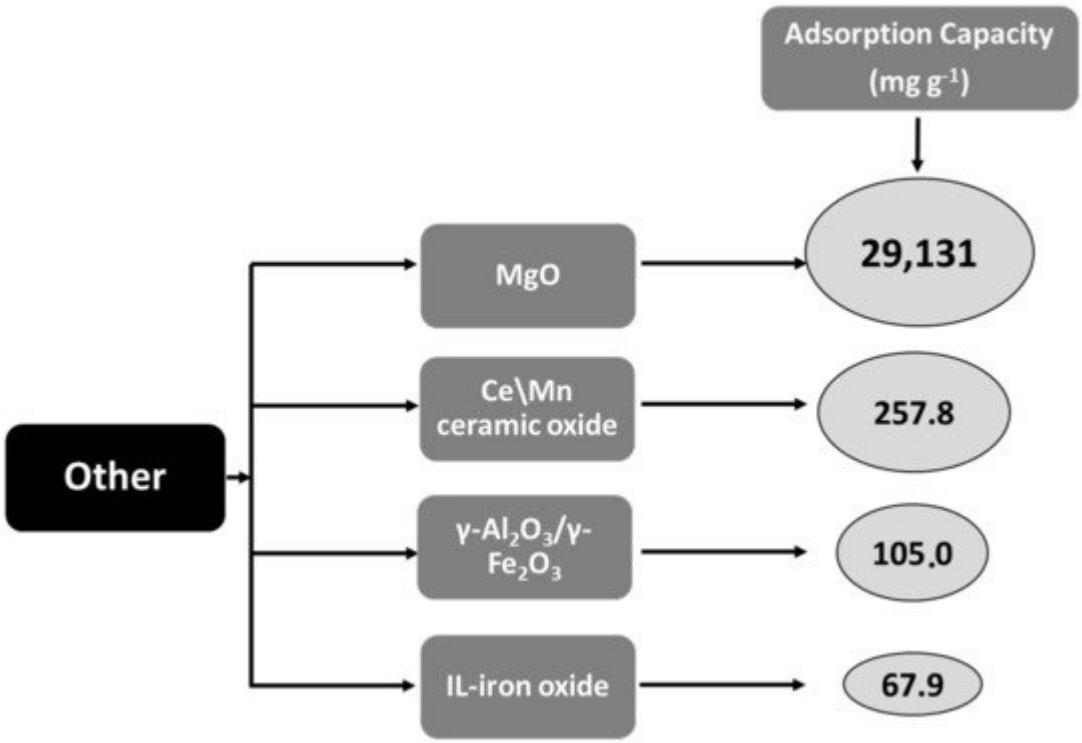

Figure 8. Schematic graph depicting maximum adsorption capacities (mg g^{-1}) of the four most efficient presented materials.

Table 2 shows the reviewed materials when employed for removal of fluoride from waters and offers evidences about their applications in water treatment. As shown in this Table, most of the recommended materials are efficient at pH values around 7. Interest was given to the application of novel materials based on GO, providing high adsorption capacity. Observing the recent literature, in the last two to three years, it is worth noting that the use of La in the modification of materials, both activated carbon as well as hybrid materials (i.e., La/Mg/Si-AC, La/MA, $LaFeO_3$ NPs) [58][75], has been successfully increased. However, by using MgO nanostructures [72], a maximum Langmuir adsorption capacity of 29,131 mg g^{-1} has been achieved, which is the greatest for any adsorbing material described until to date.

Results from the regeneration experiments performed on most of the materials reviewed, in order to test the usability of the adsorbents, showed that all of the materials can be recycled from three to six cycles. This is

considered as not very efficient, since nowadays in the production of materials almost 20 cycles of regeneration are feasible. Therefore, in this area there is more work to be done.

Many of the reviewed articles presented results on the adsorption thermodynamic behavior of the materials studied in order to indicate the feasibility of the adsorption processes. The thermodynamic parameter which reflects whether the process is spontaneous is the ΔG°, which is related to the equilibrium constant of the reaction. A spontaneous reaction releases free energy, and so the sign of ΔG° is negative. If the Gibbs energy of the process is favourable (negative), the process is enhanced at higher temperatures [51][52]. ΔH° contributes to the Gibbs energy. Exothermic adsorption processes have ΔH° < 0, and are considered endothermic when ΔH° > 0 [79]. Therefore, a rise in the adsorption capability with a temperature increase implies an endothermic adsorption procedure, while a decrease in the adsorption capacity with a temperature increase suggests an exothermic process [79][80]. Comparing the studies referred in this review article (**Table 2**) reveals that the only absorbents that provided negative ΔG° and ΔH° values were the MgO [72] and $LaFeO_3$ NPs [78]. The majority of the compared adsorbents indicate that the adsorption process was spontaneous (based on the negative values of Gibbs free energy, and the 75% provided adsorption of an endothermic nature). There is only one study in this review that presented a positive value of ΔG°, namely the GO/ES adsorbent [64], indicating that it undergoes a physio-sorption process.

Table 2. Novel carbon-based and nanostructured materials utilized for the removal of fluoride from waters. Comparison of their basic characteristics.

Adsorbent	pH	Adsorbent Dosage (g L^{-1})	Time (min)	Adsorption Capacity (mg g^{-1})	Regeneration (Cycles)	ΔG° (kJ mol^{-1}) (at 303 K)	ΔH° (kJ mol^{-1})	Ref.
Activated Carbon Based Adsorbents								
Zr-ACF	7.0	2.0	30	28.50	-	<0	>0	[50]
ACAS	6.0	19.0	60	1.20	-	-	-	[54]
AC-CMCSL	4.5	15.0	70	2.01	-	−0.20576	+22.6	[55]
La/Mg/Si-AC	8.0	0.2	150	220.5	5	-1.41×10^4 (at 308 K)	$+7.5 \times 10^3$	[56]
Graphene Oxide Based Adsorbents								
GO/Al_2O_3	6.0	8.0	90	6.30	4	−2.32	+24.6	[62]
GO–Al–O(OH)	7.0	2.0	60	51.42	-	−5.84	+21.4	[63]
GO/ES	-	0.05	120	56.0	-	0.1865 (at 298 K)	−12.7	[64]

Adsorbent	pH	Adsorbent Dosage (g L^{-1})	Time (min)	Adsorption Capacity (mg g^{-1})	Regeneration (Cycles)	ΔG° (kJ mol^{-1}) (at 303 K)	ΔH° (kJ mol^{-1})	Ref.
ZIGCS	4.0	2.0	60	175.0	5	−0.045 (at 308 K)	+30.6	[65]
Carbon Nanotubes Based Adsorbents								
HA-MWCNTs	7.0	2.0	120	39.22	-	−1.964	+6.4	[67]
Other Adsorbents								
SRH	8.0	4.0	60	6.0	4	+2.6	+2.6	[68]
Fe@BDC & Fe@ABDC MOF	6.6	0.1	60	4.90 & 4.92	6	+0.6 & +1.2	+0.6 & +1.2	[69]
KBNPs	6.5	6.0	120	1.72	-	-	-	[70]
Ce\Mn ceramic oxide	7.0	-	15	257.8	-	-	-	[71]
MgO	6.7	0.2	60	29,131	5	−47.6	−47.6	[72]
La/MA	6.0	2.0	60	26.45	5	+ 3.9	+3.9	[73]
IL-iron oxide	8.0	0.06	30	67.9	3	+6.6	+6.6	[74]
γ-Al_2O_3/γ-Fe_2O_3	7.0	1.0	15	105.04	5	+14.4	+14.4	[75]
MOF-801	-	1.0	120	17.33	4	-	-	[76]
BC-ICP	7.0	1.0	-	5.10	-	+2.3	+2.3	[77]
$LaFeO_3$ NPs	5.0	0.9	60	2.58	-	−0.51	−0.51	[78]

1. Barghouthi, Z.; Amereih, S. Spectrophotometric Determination of Fluoride in Groundwater Using Resorcin Blue Complexes. Am. J. Anal. Chem. 2012, 3, 651–655.
2. Chavali, R.; Gunda, N.S.K.; Naicker, S.; Mitra, S.K. Rapid detection of fluoride in potable water using a novel fluorogenic compound 7-O-tert-butyldiphenylsilyl-4-methylcoumarin. Anal. Chem. Res. 2015, 6, 26–31.
3. Prematilaka, R.W.; Liyanagedera, N.D. Fluoride in Drinking Water and Nanotechnological Approaches for Eliminating Excess Fluoride. J. Nanotechnol. 2019, 2019, 1–15.
4. Arya, S.; Subramani, T.; Vennila, G.; Karunanidhi, D. Health risks associated with fluoride intake from rural drinking water supply and inverse mass balance modeling to decipher hydrogeochemical processes in Vattamalaikarai River basin, South India. Environ. Geochem. Health 2021, 43, 705–716.
5. Singh, J.; Singh, P.; Singh, A. Fluoride ions vs removal technologies: A study. Arab. J. Chem. 2016, 9, 815–824.

6. Grönwall, J.; Danert, K. Regarding Groundwater and Drinking Water Access through A Human Rights Lens: Self-Supply as A Norm. Water 2020, 12, 419.
7. Yadav, K.K.; Kumar, S.; Pham, Q.B.; Gupta, N.; Rezania, S.; Kamyab, H.; Yadav, S.; Vymazal, J.; Kumar, V.; Tri, D.Q.; et al. Fluoride contamination, health problems and remediation methods in Asian groundwater: A comprehensive review. Ecotoxicol. Environ. Saf. 2019, 182, 109362.
8. Ndé-Tchoupé, A.I.; Tepong-Tsindé, R.; Lufingo, M.; Pembe-Ali, Z.; Lugodisha, I.; Mureth, R.I.; Nkinda, M.; Marwa, J.; Gwenzi, W.; Mwamila, T.B.; et al. White Teeth and Healthy Skeletons for All: The Path to Universal Fluoride-Free Drinking Water in Tanzania. Water 2019, 11, 131.
9. Rasool, A.; Farooqi, A.; Xiao, T.; Ali, W.; Noor, S.; Abiola, O.; Ali, S.; Nasim, W. A review of global outlook on fluoride contamination in groundwater with prominence on the Pakistan current situation. Environ. Geochem. Health 2018, 40, 1265–1281.
10. Wang, H.; He, H.; Wang, H.; Zhou, Z.; Yu, C. Trends of fluoride control in China. Environ. Earth Sci. 2019, 78, 580.
11. Kisku, G.C.; Sahu, P. Fluoride Contamination and Health Effects: An Indian Scenario. Environ. Concerns Sustain. Dev. 2019, 213–233.
12. Yadav, K.K.; Gupta, N.; Kumar, V.; Khan, S.; Kumar, A. A review of emerging adsorbents and current demand for defluoridation of water: Bright future in water sustainability. Environ. Int. 2018, 111, 80–108.
13. He, Z.; Liu, R.; Xu, J.; Liu, H.; Qu, J. Defluoridation by Al-based coagulation and adsorption: Species transformation of aluminum and fluoride. Sep. Purif. Technol. 2015, 148, 68–75.
14. Gong, W.-X.; Qu, J.-H.; Liu, R.-P.; Lan, H.-C. Effect of aluminum fluoride complexation on fluoride removal by coagulation. Colloids Surf. A Physicochem. Eng. Asp. 2012, 395, 88–93.
15. Tolkou, A.K.; Mitrakas, M.; Katsoyiannis, I.A.; Ernst, M.; Zouboulis, A.I. Fluoride removal from water by composite Al/Fe/Si/Mg pre-polymerized coagulants: Characterization and application. Chemosphere 2019, 231, 528–537.
16. Alhassan, S.I.; Huang, L.; He, Y.; Yan, L.; Wu, B.; Wang, H. Fluoride removal from water using alumina and aluminum-based composites: A comprehensive review of progress. Crit. Rev. Environ. Sci. Technol. 2020, 2020, 1–35.
17. Jagtap, S.; Yenkie, M.K.; Labhsetwar, N.; Rayalu, S. Fluoride in Drinking Water and Defluoridation of Water. Chem. Rev. 2012, 112, 2454–2466.
18. Kumar, P.S.; Suganya, S.; Srinivas, S.; Priyadharshini, S.; Karthika, M.; Sri, R.K.; Swetha, V.; Naushad, M.; Lichtfouse, E. Treatment of fluoride-contaminated water. A review. Environ. Chem. Lett. 2019, 17, 1707–1726.

19. Van der Bruggen, B.; Mänttäri, M.; Nyström, M. Drawbacks of applying nanofiltration and how to avoid them: A review. Sep. Purif. Technol. 2008, 63, 251–263.
20. Fito, J.; Said, H.; Feleke, S.; Worku, A. Fluoride removal from aqueous solution onto activated carbon of Catha edulis through the adsorption treatment technology. Environ. Syst. Res. 2019, 8, 1–10.
21. Zarrabi, M.; Samadi, M.T.; Sepehr, M.N.; Ramhormozi, S.M.; Azizian, S.; Amrane, A. Removal of Fluoride Ions by Ion Exchange Resin: Kinetic and Equilibrium Studies. Environ. Eng. Manag. J. 2014, 13, 205–214.
22. Prabhu, S.M.; Meenakshi, S. Synthesis of metal ion loaded silica gel/chitosan biocomposite and its fluoride uptake studies from water. J. Water Process. Eng. 2014, 3, 144–150.
23. Varaprasad, K.; Nunez, D.; Yallapu, M.M.; Jayaramudu, T.; Elgueta, E.; Oyarzun, P. Nano-hydroxyapatite polymeric hydrogels for dye removal. RSC Adv. 2018, 8, 18118–18127.
24. Tor, A.; Danaoglu, N.; Arslan, G.; Cengeloglu, Y. Removal of fluoride from water by using granular red mud: Batch and column studies. J. Hazard. Mater. 2009, 164, 271–278.
25. Kemer, B.; Ozdes, D.; Gundogdu, A.; Bulut, V.N.; Duran, C.; Soylak, M. Removal of fluoride ions from aqueous solution by waste mud. J. Hazard. Mater. 2009, 168, 888–894.
26. Fujita, S.; Suzuki, A. Electrical Conduction in Graphene and Nanotubes; John Wiley & Sons: Hoboken, NJ, USA, 2013; ISBN 9783527411.
27. Geethamani, C.; Ramesh, S.; Gandhimathi, R.; Nidheesh, P. Alkali-treated fly ash for the removal of fluoride from aqueous solutions. Desalination Water Treat. 2013, 52, 3466–3476.
28. Delgadillo-Velasco, L.; Hernández-Montoya, V.; Cervantes, F.J.; Montes-Morán, M.A.; Lira-Berlanga, D. Bone char with antibacterial properties for fluoride removal: Preparation, characterization and water treatment. J. Environ. Manag. 2017, 201, 277–285.
29. Ndé-Tchoupé, A.I.; Nanseu-Njiki, C.P.; Hu, R.; Nassi, A.; Noubactep, C.; Licha, T. Characterizing the reactivity of metallic iron for water defluoridation in batch studies. Chemosphere 2019, 219, 855–863.
30. Khandare, D.; Mukherjee, S. A Review of Metal oxide Nanomaterials for Fluoride decontamination from Water Environment. Mater. Today Proc. 2019, 18, 1146–1155.
31. Suriyaraj, S.P.; Selvakumar, R. Advances in nanomaterial based approaches for enhanced fluoride and nitrate removal from contaminated water. RSC Adv. 2016, 6, 10565–10583.
32. Yahyavi, H.; Kaykhaii, M.; Mirmoghaddam, M. Recent Developments in Methods of Analysis for Fluoride Determination. Crit. Rev. Anal. Chem. 2015, 46, 106–121.

33. Radić, J.; Bralić, M.; Kolar, M.; Genorio, B.; Prkić, A.; Mitar, I. Development of the New Fluoride Ion-Selective Electrode Modified with FexOy Nanoparticles. Molecules 2020, 25, 5213.
34. Hussain, I.; Ahamad, K.U.; Nath, P. Low-Cost, Robust, and Field Portable Smartphone Platform Photometric Sensor for Fluoride Level Detection in Drinking Water. Anal. Chem. 2016, 89, 767–775.
35. Mohapatra, M.; Anand, S.; Mishra, B.; Giles, D.E.; Singh, P. Review of fluoride removal from drinking water. J. Environ. Manag. 2009, 91, 67–77.
36. Bhatnagar, A.; Kumar, E.; Sillanpää, M. Fluoride removal from water by adsorption-A review. Chem. Eng. J. 2011, 171, 811–840.
37. Dhillon, A.; Nair, M.; Kumar, D. Analytical methods for determination and sensing of fluoride in biotic and abiotic sources: A review. Anal. Methods 2016, 8, 5338–5352.
38. Jin, H.; Ji, Z.; Yuan, J.; Li, J.; Liu, M.; Xu, C.; Dong, J.; Hou, P.; Hou, S. Research on removal of fluoride in aqueous solution by alumina-modified expanded graphite composite. J. Alloys Compd. 2015, 620, 361–367.
39. Larsen, M.; Pearce, E.; Ravnholt, G. The effectiveness of bone char in the defluoridation of water in relation to its crystallinity, carbon content and dissolution pattern. Arch. Oral Biol. 1994, 39, 807–816.
40. Kennedy, A.M.; Arias-Paic, M. Fixed-Bed Adsorption Comparisons of Bone Char and Activated Alumina for the Removal of Fluoride from Drinking Water. J. Environ. Eng. 2020, 146, 04019099.
41. Alkurdi, S.S.; Al-Juboori, R.A.; Bundschuh, J.; Hamawand, I. Bone char as a green sorbent for removing health threatening fluoride from drinking water. Environ. Int. 2019, 127, 704–719.
42. Nigri, E.M.; Santos, A.L.A.; Bhatnagar, A.; Rocha, S.D.F. Chemical Regeneration of Bone Char Associated With A Continuous System for Defluoridation of Water. Braz. J. Chem. Eng. 2019, 36, 1631–1643.
43. Nigri, E.M.; Bhatnagar, A.; Rocha, S.D.F. Thermal regeneration process of bone char used in the fluoride removal from aqueous solution. J. Clean. Prod. 2017, 142, 3558–3570.
44. Kanouo, B.M.D.; Fonteh, M.F.; Ngambo, S.P. Development of a low cost household bone-char defluoridation filter. Int. J. Biol. Chem. Sci. 2020, 14, 1921–1927.
45. Collivignarelli, M.C.; Abbà, A.; Miino, M.C.; Torretta, V.; Rada, E.C.; Caccamo, F.M.; Sorlini, S. Adsorption of Fluorides in Drinking Water by Palm Residues. Sustainability 2020, 12, 3786.
46. Herath, H.M.A.S.; Kawakami, T.; Tafu, M. The Extremely High Adsorption Capacity of Fluoride by Chicken Bone Char (CBC) in Defluoridation of Drinking Water in Relation to Its Finer Particle Size for Better Human Health. Healthcares 2018, 6, 123.

47. Kikuchi, M.; Arioka, Y.; Tafu, M.; Irie, M. Changes in fluoride removal ability of chicken bone char with changes in calcination time. Int. J. Ceram. Eng. Sci. 2020, 2, 83–91.
48. AlOthman, Z.A.; Habila, M.; Ali, R.; Ghafar, A.A.; El-din Hassounab, M.S. Valorization of two waste streams into activated carbon and studying its adsorption kinetics, equilibrium isotherms and thermodynamics for methylene blue removal. Arab. J. Chem. 2014, 7, 1148–1158.
49. Gallios, G.P.; Tolkou, A.K.; Katsoyiannis, I.A.; Stefusova, K.; Vaclavikova, M.; Deliyanni, E.A. Adsorption of Arsenate by Nano Scaled Activated Carbon Modified by Iron and Manganese Oxides. Sustainability 2017, 9, 1684.
50. Li, Y.; Zhang, C.; Jiang, Y.; Wang, T.-J. Electrically enhanced adsorption and green regeneration for fluoride removal using Ti(OH)4-loaded activated carbon electrodes. Chemosphere 2018, 200, 554–560.
51. Pang, T.; Chan, T.S.A.; Jande, Y.A.C.; Shen, J. Removal of fluoride from water using activated carbon fibres modified with zirconium by a drop-coating method. Chemosphere 2020, 255, 126950.
52. Li, Y.-H.; Di, Z.; Ding, J.; Wu, D.; Luan, Z.; Zhu, Y. Adsorption thermodynamic, kinetic and desorption studies of Pb2+ on carbon nanotubes. Water Res. 2005, 39, 605–609.
53. Khan, Z.H.; Gao, M.; Qiu, W.; Islam, S.; Song, Z. Mechanisms for cadmium adsorption by magnetic biochar composites in an aqueous solution. Chemosphere 2020, 246, 125701.
54. Gao, H.; Kan, T.; Zhao, S.; Qian, Y.; Cheng, X.; Wu, W.; Wang, X.; Zheng, L. Removal of anionic azo dyes from aqueous solution by functional ionic liquid cross-linked polymer. J. Hazard. Mater. 2013, 261, 83–90.
55. Tefera, N.; Mulualem, Y.; Fito, J. Adsorption of Fluoride from Aqueous Solution and Groundwater onto Activated Carbon of Avocado Seeds. Water Conserv. Sci. Eng. 2020, 5, 187–197.
56. Dehghani, M.H.; Farhang, M.; Alimohammadi, M.; Afsharnia, M.; McKay, G. Adsorptive removal of fluoride from water by activated carbon derived from CaCl2-modified Crocus sativus leaves: Equilibrium adsorption isotherms, optimization, and influence of anions. Chem. Eng. Commun. 2018, 205, 955–965.
57. Kim, M.; Choong, C.E.; Hyun, S.; Park, C.M.; Lee, G. Mechanism of simultaneous removal of aluminum and fluoride from aqueous solution by La/Mg/Si-activated carbon. Chemosphere 2020, 253, 126580.
58. Lin, Y.-J.; Cao, W.-Z.; Ouyang, T.; Mohan, S.; Chang, C.-T. Adsorption mechanism of magnetic nanoparticles doped with graphene oxide and titanium nanotubes for As(III) removal. Materialia 2018, 3, 79–89.

59. Molla, A.; Li, Y.; Mandal, B.; Kang, S.G.; Hur, S.H.; Chung, J.S. Selective adsorption of organic dyes on graphene oxide: Theoretical and experimental analysis. Appl. Surf. Sci. 2019, 464, 170–177.
60. Liu, H.; Zhang, F.; Peng, Z. Adsorption mechanism of Cr(VI) onto GO/PAMAMs composites. Sci. Rep. 2019, 9, 1–12.
61. Tolkou, A.K.; Zouboulis, A.I. Graphene Oxide/Fe-Based Composite Pre-Polymerized Coagulants: Synthesis, Characterization, and Potential Application in Water Treatment. C J. Carbon Res. 2020, 6, 44.
62. Guan, C.; Lv, X.; Han, Z.; Chen, C.; Xu, Z.; Liu, Q. The adsorption enhancement of graphene for fluorine and chlorine from water. Appl. Surf. Sci. 2020, 516, 146157.
63. Xu, N.; Li, S.; Li, W.; Liu, Z. Removal of Fluoride by Graphene Oxide/Alumina Nanocomposite: Adsorbent Preparation, Characterization, Adsorption Performance and Mechanisms. ChemistrySelect 2020, 5, 1818–1828.
64. Barathi, M.; Kumar, S.K.; Kumar, C.U.; Rajesh, N.P. Graphene oxide–aluminium oxyhydroxide interaction and its application for the effective adsorption of fluoride. RSC Adv. 2014, 4, 53711–53721.
65. Nor, N.M.; Kamil, N.H.N.; Mansor, A.I.; Maarof, H.I. Adsorption Analysis of Fluoride Removal Using Graphene Oxide/Eggshell Adsorbent. Indones. J. Chem. 2020, 20, 579–586.
66. Prathibha, C.; Biswas, A.; Chunduri, L.A.; Reddy, S.K.; Loganathan, P.; Kalaruban, M.; Venkatarmaniah, K. Zr(IV) functionalized graphene oxide anchored sand as potential and economic adsorbent for fluoride removal from water. Diam. Relat. Mater. 2020, 109, 108081.
67. Ruan, Z.; Tian, Y.; Ruan, J.; Cui, G.; Iqbal, K.; Iqbal, A.; Ye, H.; Yang, Z.; Yan, S. Synthesis of hydroxyapatite/multi-walled carbon nanotubes for the removal of fluoride ions from solution. Appl. Surf. Sci. 2017, 412, 578–590.
68. Pillai, P.; Dharaskar, S.; Shah, M.; Sultania, R. Determination of fluoride removal using silica nano adsorbent modified by rice husk from water. Groundw. Sustain. Dev. 2020, 11, 100423.
69. Jeyaseelan, A.; Naushad, M.; Ahamad, T.; Viswanathan, N. Design and development of amine functionalized iron based metal organic frameworks for selective fluoride removal from water environment. J. Environ. Chem. Eng. 2021, 9, 104563.
70. Annan, E.; Nyankson, E.; Agyei-Tuffour, B.; Armah, S.K.; Nkrumah-Buandoh, G.; Hodasi, J.A.M.; Oteng-Peprah, M. Synthesis and Characterization of Modified Kaolin-Bentonite Composites for Enhanced Fluoride Removal from Drinking Water. Adv. Mater. Sci. Eng. 2021, 2021, 1–12.
71. Vences-Alvarez, E.; Flores-Arciniega, J.L.; Flores-Zuñiga, H.; Rangel-Mendez, J.R. Fluoride removal from water by ceramic oxides from cerium and manganese solutions. J. Mol. Liq. 2019,

286, 110880.

72. Borgohain, X.; Boruah, A.; Sarma, G.K.; Rashid, H. Rapid and extremely high adsorption performance of porous MgO nanostructures for fluoride removal from water. J. Mol. Liq. 2020, 305, 112799.
73. He, Y.; Zhang, L.; An, X.; Wan, G.; Zhu, W.; Luo, Y. Enhanced fluoride removal from water by rare earth (La and Ce) modified alumina: Adsorption isotherms, kinetics, thermodynamics and mechanism. Sci. Total Environ. 2019, 688, 184–198.
74. Pillai, P.; Dharaskar, S.; Sinha, M.K.; Sillanpää, M.; Khalid, M. Iron oxide nanoparticles modified with ionic liquid as an efficient adsorbent for fluoride removal from groundwater. Environ. Technol. Innov. 2020, 19, 100842.
75. Roy, A. Microwave-assisted synthesis and characterization of γ-Al2O3/γ-Fe2O3 composite and evaluating its efficiency in fluoride removal. Colloids Surf. A Physicochem. Eng. Asp. 2021, 608, 125574.
76. Tan, T.L.; Krusnamurthy, P.A.; Nakajima, H.; Rashid, S.A. Adsorptive, kinetics and regeneration studies of fluoride removal from water using zirconium-based metal organic frameworks. RSC Adv. 2020, 10, 18740–18752.
77. Wang, Z.; Su, J.; Hu, X.; Ali, A.; Wu, Z. Isolation of biosynthetic crystals by microbially induced calcium carbonate precipitation and their utilization for fluoride removal from groundwater. J. Hazard. Mater. 2021, 406, 124748.
78. Mesbah, M.; Hamedshahraki, S.; Ahmadi, S.; Sharifi, M.; Igwegbe, C.A. Hydrothermal synthesis of LaFeO3 nanoparticles adsorbent: Characterization and application of error functions for adsorption of fluoride. MethodsX 2020, 7, 100786.
79. Al-Ghouti, M.A.; Al-Absi, R.S. Mechanistic understanding of the adsorption and thermodynamic aspects of cationic methylene blue dye onto cellulosic olive stones biomass from wastewater. Sci. Rep. 2020, 10, 1–18.
80. Thomas, J.M. The existence of endothermic adsorption. J. Chem. Educ. 1961, 38, 138.